Physics Letters B 695 (2011) 13–18

Contents lists available at ScienceDirect

Physics Letters B

www.elsevier.com/locate/physletb

Restricting UHECRs and cosmogenic neutrinos with Fermi-LAT

V. Berezinsky [a], A. Gazizov [a,b], M. Kachelrieß [b,*], S. Ostapchenko [b,c]

[a] INFN, Laboratori Nazionali del Gran Sasso, I-67010 Assergi (AQ), Italy
[b] Institutt for Fysikk, NTNU, Trondheim, Norway
[c] D.V. Skobeltsyn Institute of Nuclear Physics, Moscow State University, Russia

ARTICLE INFO

Article history:
Received 14 June 2010
Received in revised form 4 November 2010
Accepted 4 November 2010
Available online 11 November 2010
Editor: S. Dodelson

Keywords:
High energy neutrinos
Ultrahigh energy cosmic rays
Diffuse gamma-ray background

ABSTRACT

Ultrahigh energy cosmic ray (UHECR) protons interacting with the cosmic microwave background (CMB) produce UHE electrons and gamma-rays that in turn initiate electromagnetic cascades on CMB and infrared photons. As a result, a background of diffuse isotropic gamma-radiation is accumulated in the energy range $E \lesssim 100$ GeV. The Fermi-LAT Collaboration has recently reported a measurement of the extragalactic diffuse background finding it less intense and softer than previously measured by EGRET. We show that this new result constrains UHECR models and the flux of cosmogenic neutrinos. In particular, it excludes models with cosmogenic neutrino fluxes detectable by existing neutrino experiments, while next-generation detectors as e.g. JEM-EUSO can observe neutrinos only for extreme parameters.

1. Introduction

The origin of ultrahigh energy cosmic rays (UHECRs) is not yet established despite more than 50 years of research. Natural candidates as UHECR primaries are extragalactic protons from astrophysical sources. In this case, interactions of UHE protons with the cosmic microwave background (CMB) leave their imprint on the UHECR energy spectrum in the form of the Greisen–Zatsepin–Kuzmin (GZK) cutoff and a pair-production dip [1].

The GZK cutoff is a steepening of the proton spectrum at the energy $E_{\rm GZK} \approx (4\text{–}5) \times 10^{19}$ eV, caused by photo-pion production on the CMB. Such a steepening has been observed by the HiRes [2] and the Auger Collaboration [3], but its real cause is still unclear.

An immediate consequence of the dominance of extragalactic protons in the CR flux and their interaction with CMB photons is the existence of ultrahigh energy ("cosmogenic") neutrinos produced by charged pion decays, as suggested first in Ref. [4].

Another signature for extragalactic protons is a pair-production dip [5,6] in the CR flux around 5×10^{18} eV, which is clearly seen in the experimental data. Photons and positrons from pion decay and $p + \gamma_{\rm CMB} \to p + e^+ + e^-$ pair-production initiate electromagnetic cascades on photons from the CMB and the extragalactic background light (EBL), dumping all the energy injected into cascade particles below the pair-production threshold at ~ 100 GeV.

Clearly, the production of neutrinos by UHE protons is thus intimately tied to the one of photons and electrons, and both depend in turn on the flux of primary cosmic rays. While UHE photons and electrons start electromagnetic cascades by scattering on photons from the EBL, neutrinos reach us suffering no collisions. Therefore, the measurement of the diffuse extragalactic gamma-ray background (EGRB) can be used to impose a strict upper limit on the possible diffuse high energy neutrino flux, as suggested first in Ref. [7].

We derive in this work an upper limit on the flux of cosmogenic neutrinos assuming that the primary UHECR particles are protons. In case that all primaries or part of them are nuclei, the cosmogenic neutrino flux is lower than for a pure proton composition [8]. Thus our assumption of a pure proton composition is justified, since we aim at deriving an *upper limit* on the cosmogenic neutrino flux. Note that the HiRes data [2] agree with a pure proton composition at $E \gtrsim 1 \times 10^{18}$ eV, while the mass composition deduced from the Auger data indicates the presence of heavier nuclei in the primary UHECR flux [3]. In the latter case, the maximally allowed cosmogenic neutrino flux would be below the upper limit derived for a pure proton primary flux in this Letter.

In the present work, we use a recently reported measurement [9] of the EGRB by Fermi-LAT to constrain UHECR models. We show that the observed fast decrease of the EGRB with energy, $J(E) \propto E^{-2.41}$, already constrains such models. In particular, versions of the dip model with strong redshift evolution contradict the Fermi data, while this model without or with weak redshift evolution remains viable. Moreover, the Fermi data allows us to derive a strong upper limit on the diffuse UHE neutrino flux. As a result, we conclude that the detection of cosmogenic neutrinos requires to increase the sensitivity of UHE neutrino experiments compared to current levels. As it is demonstrated below, the maxi-

* Corresponding author.
E-mail address: Michael.Kachelriess@ntnu.no (M. Kachelrieß).

0370-2693
doi:10.1016/j.physletb.2010.11.019

mal energy density of cascade radiation $\omega_{\rm cas}^{\rm max} \approx 5.8\times 10^{-7}$ eV/cm^3 allowed by the Fermi-LAT data can be used to select viable UHECR models without explicitly calculating electromagnetic cascade processes.

2. Analytical calculations

The two basic processes driving an electromagnetic cascade are pair production (PP) $\gamma\gamma_{\rm b}\to e^+e^-$ and inverse Compton (IC) scattering $e^\pm\gamma_{\rm b}\to e^\pm\gamma$ on background photons $\gamma_{\rm b}$. The cascade develops very fast with a minimal interaction length $l_{\rm int}(E)\sim 10$ kpc until it reaches the pair creation threshold. From that point on, electrons emit photons in the Thomson regime while photons stop interacting. Their spectrum can be estimated analytically [7,10] in terms of the production rate of the cascade photons $Q_\gamma^{\rm cas}(E)$ per unit volume as

$$Q_\gamma^{\rm cas}(E)=\begin{cases} K(E/\varepsilon_X)^{-3/2} & \text{for } E\leqslant\varepsilon_X,\\ K(E/\varepsilon_X)^{-2} & \text{for } \varepsilon_X\leqslant E\leqslant\varepsilon_a,\end{cases} \tag{1}$$

with a steepening at $E>\varepsilon_a$. Here, ε_a is the minimal absorption energy of a cascade photon scattering on the EBL, and ε_X is the energy of a photon emitted by an electron/positron ($e_X+\gamma\to e'+\gamma_X$), which is in turn produced by a photon γ_a (via $\gamma_a+\gamma_{\rm EBL}\to e_X^+ + e_{\bar X}^-$) with the minimal absorption energy ε_a. The energy spectrum (1) of the cascade radiation typically extends up to ~ 100 GeV. The constant K in Eq. (1) defines the normalization of the production rate via $K=Q_\gamma^{\rm cas}(\varepsilon_X)$. The two energies ε_a and ε_X are related to each other as $\varepsilon_X=1/3(\varepsilon_a/m_e)^2\varepsilon_{\rm cmb}$ [7,10], where $\varepsilon_{\rm cmb}=6.35\times 10^{-4}$ eV is the mean energy of CMB photons.

We can account for the absorption of cascade photons on the EBL, integrating their production rate $Q_\gamma^{\rm cas}(E)$ over the volume of the universe,

$$J_{\rm abs}^{\rm cas}(E)=\frac{c}{4\pi}\int dV\,\frac{Q_\gamma^{\rm cas}(E)}{4\pi r^2 c}\exp\left(-\frac{r}{l_{\rm int}(E)}\right). \tag{2}$$

Integrating the rate from $r=0$ up to cH_0^{-1} we obtain the relation between the absorbed flux $J_{\rm abs}^{\rm cas}(E)$ and the unabsorbed flux $J_\gamma^{\rm cas}(E)$,

$$J_{\rm abs}^{\rm cas}(E)=J_\gamma^{\rm cas}(E)\frac{l_{\rm int}(E)}{cH_0^{-1}}\left[1-\exp\left(-\frac{cH_0^{-1}}{l_{\rm int}(E)}\right)\right]. \tag{3}$$

Here, H_0 denotes the present value of the Hubble parameter.

The cascade energy density $\omega_{\rm cas}$ at the present epoch is calculated as

$$\omega_{\rm cas}=\frac{4\pi}{c}\int dE\,E\,J_{\rm abs}^{\rm cas}(E). \tag{4}$$

In Fig. 1, we show the measurement of the EGRB by Fermi-LAT [9] (black circles with error bars) together with the maximally allowed photon flux (solid red line) derived analytically. More precisely, we have determined the maximally allowed photon flux requiring that the curve just touches the lower end of the error bars of the Fermi-LAT data. The corresponding bound on the cascade energy density is $\omega_{\rm cas}^{\rm max}=5.8\times 10^{-7}$ eV/cm^3.

The bound on $\omega_{\rm cas}^{\rm max}$ derived by us can be used to select in a simple way viable UHECR models.

We limit our consideration to pure proton-composition models, which are described by the generation index α_g, the maximum acceleration energy $E_{\rm max}$ and the cosmological evolution of the sources parametrized by $(1+z)^m$ with fixed m and maximal redshift $z_{\rm max}$. The quantity of interest, the space density of protons $n_p(E,z)$ at each cosmological epoch, is calculated as in Ref. [6] in the continuous energy-loss approximation. To evaluate the role of

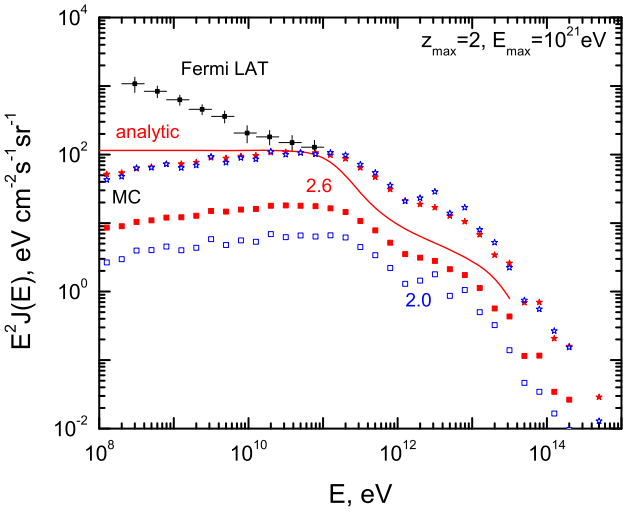

Fig. 1. Fermi-LAT EGRB spectrum (black circles with error bars) in comparison with maximally allowed fluxes given by analytical (solid red line) and MC calculations (red stars for $\alpha_g=2.6$, and blue stars $\alpha_g=2.0$). All three curves are normalized by the highest energy point of the Fermi spectrum. The MC EGRB fluxes are calculated for the following values of the parameters: $E_{\rm max}=10^{21}$ eV, $z_{\rm max}=2$, $m=0$ and $\alpha_g=2.6$ or 2.0. Also shown two MC spectra with the same parameters as above, but normalized to the HiRes proton spectrum (red boxes for $\alpha_g=2.6$ and blue boxes for $\alpha_g=2.0$). The plot illustrates the universality of the cascade spectrum and reasonably good agreement between MC and analytical results. (For interpretation of the references to color in this figure legend, the reader is referred to the web version of this Letter.)

fluctuations in $p+\gamma\to\pi+$all scattering, the density of protons in Ref. [6] was computed also solving the kinetic equation (16). It was found that for $E_{\rm max}=1\times 10^{21}$ eV both methods give practically identical results, while for $E_{\rm max}=1\times 10^{23}$ eV the difference does not exceed 15%. In the calculations of this work, the UHE proton fluxes at $z=0$ are normalized to fit the HiRes spectra [2].

The UHE diffuse neutrino flux at highest energies depends mainly on α_g and $E_{\rm max}$. The generation index is limited as $2.0\lesssim\alpha_g\lesssim 2.7$, by the following reason: Let us choose first the minimum possible index $\alpha_g=2.0$. In this case, the calculated extragalactic UHECR flux is very flat and can explain the observed spectrum only above $E\sim(0.5\text{–}1)\times 10^{19}$ eV, i.e. above the ankle. Increasing α_g decreases the predicted transition energy between galactic and extragalactic UHECRs, until for $\alpha_g\approx 2.6\text{–}2.7$ this energy becomes lower than 1×10^{18} eV, where, as observations show, heavy nuclei dominate.

UHECR models allowed by Fermi-LAT data, i.e. leading to a cascade energy density $\omega_{\rm cas}$ below $\omega_{\rm cas}^{\rm max}=5.8\times 10^{-7}$ eV/cm^3, are characterized by a low value of $E_{\rm max}$ or weak source evolution. For each given model, we calculate $\omega_{\rm cas}$ as

$$\omega_{\rm cas}=\int\frac{dt\,dE}{1+z}\,E\beta_{0,\rm em}\big[(1+z)E\big]n_p(E,z), \tag{5}$$

where n_p is the (physical) density of protons at redshift z, $\beta_0(E)=(1/E)(dE/dt)$ is the relative rate of energy loss of a proton with energy E at $z=0$, and $\beta_{0,\rm em}$ denotes the relative rate of energy injected by protons into electromagnetic cascades due to pair production and pion production ($p\gamma\to\pi^\pm\to e^\pm$ and $p\gamma\to\pi^0\to\gamma$) at $z=0$. In Table 1, we report the numerical values obtained for $\omega_{\rm cas}$ for different values of the maximal energy of acceleration $E_{\rm max}$, exponents α_g of the generation spectrum and the maximal redshift $z_{\rm max}$. The UHE proton fluxes at $z=0$ are normalized to the HiRes data [2]. In Table 1 we show also the ratio of the contribution from pair production to the one from pion production. The cases with different α_g in Table 1 correspond to different transi-

Table 1
The energy density $\omega_{\rm cas}$ of the cascade radiation produced by UHE protons normalized to HiRes data.

m	$E_{\rm max}$	α_g	$z_{\rm max}$	$\omega_{\rm cas}$ [eV/cm^3]	$\omega_{\rm cas}^{e^+e^-}/\omega_{\rm cas}^{\pi}$
No evolution, allowed models					
0	10^{21}	2.0	2	$4.0\cdot10^{-8}$	2.41
0	10^{21}	2.7	2	$1.2\cdot10^{-7}$	24.5
0	10^{22}	2.0	2	$5.1\cdot10^{-8}$	1.2
0	10^{22}	2.7	2	$1.2\cdot10^{-7}$	20.8
0	10^{22}	2.0	3	$5.5\cdot10^{-8}$	1.2
0	10^{22}	2.7	3	$1.4\cdot10^{-7}$	22.0
With evolution, allowed models					
2.5	10^{22}	2.0	4	$2.7\cdot10^{-7}$	1.46
3	10^{21}	2.5	2	$4.3\cdot10^{-7}$	14.7
3	10^{22}	2.4	3	$5.8\cdot10^{-7}$	8.4
Models excluded by $\omega_{\rm cas}$					
3.5	10^{23}	2.3	3	$7.4\cdot10^{-7}$	4.9
4	10^{21}	2.5	2	$8.6\cdot10^{-7}$	15.3
4	10^{22}	2.0	3	$7.6\cdot10^{-7}$	1.5

tion energies from galactic to extragalactic cosmic rays, increasing from $E\sim1\times10^{18}$ eV for $\alpha_g=2.6$ to $E\sim5\times10^{18}$ eV for $\alpha_g=2.0$. Table 1 gives examples of UHECR models that are allowed and that are forbidden by the Fermi-LAT data.

The upper part of Table 1 (no-evolution case) presents the allowed models with $\omega_{\rm cas}<5.8\times10^{-7}$ eV/cm^3. In the two lower parts the cosmological evolution of UHECR sources is included, assuming that the product of the comoving source density n_s and the source luminosity L_s evolves as $n_s(z)L_s(z)=n_0L_0(1+z)^m$. The middle part contains both allowed and marginally allowed evolutionary models. The large neutrino fluxes at highest energies, favorable for detection by the JEM-EUSO instrument and by radio methods, are expected in the models with flat spectra ($\alpha_g=2.0$) and large $E_{\rm max}$. Examples of such models allowed by $\omega_{\rm cas}$ are also given in Table 1, most notably the one in the first row of the middle part. On the other hand, large neutrino fluxes at energies up to 1×10^{17} eV, which are favorable for IceCube detection, do not require large $E_{\rm max}$ but strong evolution. One can find such models in Table 1, too, among the allowed models. In the lower part of Table 1 three examples for evolutionary models forbidden by the Fermi-LAT data are shown.

Note that apart from the cascade radiation, one should expect various additional contributions to the measured Fermi flux and these contributions lower $\omega_{\rm cas}^{\rm max}$ further. Among them are photons from unresolved [11] or dead [12] active galactic nuclei (AGN) and from other galaxies. Dark matter annihilations and/or decays in the extended DM galactic halo or beyond can give another contribution to the Fermi flux. Subtracting these processes would strengthen the upper limit on the neutrino flux derived below, and thus our result is conservative. On the other hand, extragalactic magnetic fields with strength above 1 nG play the opposite role: High-energy cascade electrons loose energy radiating predominantly synchrotron photons, which are not detected by Fermi-LAT and thus the energies of these electrons do not contribute to $\omega_{\rm cas}$. We show below that in the case of magnetic field strengths less than 1 nG this correction on the limit for UHE neutrino flux is small.

3. Monte Carlo simulation

In addition to the analytical treatment, we obtain the EGRB spectrum based on a Monte Carlo simulation of the cascade development. We generate CR sources from a homogeneous source distribution up to a maximal redshift $z_{\rm max}$. Assuming the proton injection spectrum in the form $dN/dE\propto E^{-\alpha_g}\vartheta(E-E_{\rm max})$, we propagate the UHE protons accelerated in the sources through the extragalactic space, using the Monte Carlo code described in [13], until their energy is below the threshold for e^+e^- pair production, $E_{\rm min}\approx10^{18}$ eV, or until they reach the Earth. For the simulation of pion production we use SOPHIA [14], while e^+e^- pairs are injected according to the continuous energy losses and their mean energy calculated in Refs. [6,15].

We follow the evolution of electromagnetic cascades using the Monte Carlo code introduced in Ref. [16] and the best-fit model of [17] for the EBL energy density. The MC procedure provides a one-dimensional description of the cascade development, taking into account the pair production and IC processes as well as adiabatic energy losses. Extragalactic magnetic fields with average strengths close to the upper limit $B\sim1$ nG have a small influence (of order 20%) on the resulting EGRB. We will discuss further this result below.

In Fig. 1, the cascade fluxes are shown for two UHECR models. The curve marked as $\alpha_g=2.6$ (red boxes) gives the cascade flux for the non-evolutionary ($m=0$) dip model [6] with $E_{\rm max}=1\times10^{21}$ eV and $z_{\rm max}=2$ normalized to HiRes data. The other curve marked as $\alpha_g=2.0$ is shown for the ankle model with a transition from galactic to extragalactic cosmic rays at 5×10^{18} eV for the same values of $E_{\rm max}$ and $z_{\rm max}$. From Fig. 1, one can see that both models are allowed by the cascade limit.

The MC simulation allows us to test the *universality* of the cascade spectrum. If a cascade is initiated by a photon or an electron of very high energy, the energy spectrum of the resulting cascade photons depends only weakly on the energy of the primary particle for a sufficiently large number of cascade steps. This universality is obviously broken for the primaries injected close enough to an observer, if the distance is of the order of the absorption length (see Eq. (2)). In Fig. 1 we plot the MC cascade spectra with $\alpha_g=2.6$ and $\alpha_g=2.0$ normalizing them by the highest energy point of the Fermi spectrum (red and blue stars in Fig. 1). The comparison of the three theoretical spectra at energies below the minimal absorption energy ε_a shows that the cascade spectrum is indeed quite universal. The shape of the cascade photon spectra from the Monte Carlo simulation agrees reasonably well with the one analytically calculated, with a somewhat harder photon flux obtained with the Monte Carlo method in the plateau region, $J(E)\propto E^{-1.95}$. As a result, the maximal cascade energy density $\omega_{\rm cas}^{\rm max}$ obtained using the Monte Carlo simulation is 30% smaller than in the analytic calculations.

In Fig. 2, we show the obtained UHECR, neutrino and photon fluxes together with data from HiRes and Fermi-LAT for the two cases $\alpha_g=2.0$ (blue) and 2.6 (red). We use again $E_{\rm max}=10^{21}$ eV, $z_{\rm max}=2$ and normalize the UHECR results to the HiRes observations. While the dip model fits the HiRes data with $\chi^2=19.5$ for d.o.f. $=19$, the ankle model cannot explain the HiRes data below 1×10^{19} eV without an additional component. Clearly, the dip scenario without evolution and with modest values of $E_{\rm max}$ and $z_{\rm max}$ is well compatible with the Fermi data (see Fig. 1). The ankle scenario with $\alpha_g=2.0$ has a lower flux of cascade gamma-radiation and is viable too.

4. The cascade bound on UHE neutrinos

This is the most general bound on the UHE neutrino flux, based only on the production of electromagnetic cascades, which inevitably accompany the production of pions responsible for the neutrino flux [7,10]. It is based on the approximate equality of the total energy release to neutrino radiation (through $p\gamma\to\pi^\pm\to\nu$) and to the cascade radiation (through $p\gamma\to\pi^\pm\to e^\pm$ and $p\gamma\to\pi^0\to\gamma$) in pion production process. The upper limit on the in-

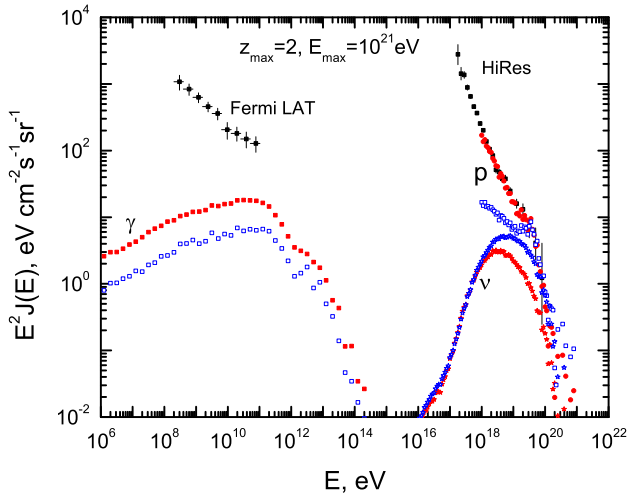

Fig. 2. Fermi-LAT data (black circles) for the EGRB and UHECR data from HiRes (dots) together with UHE neutrino (stars) and photon (boxes) fluxes for $E_{\max} = 10^{21}$ eV, $z_{\max} = 2$, $m = 0$ and $\alpha_g = 2.0$ (blue, open) and $\alpha_g = 2.6$ (red, filled symbols). (For interpretation of the references to color in this figure legend, the reader is referred to the web version of this Letter.)

tegral flux $J_\nu\ (> E)$ of neutrinos of all flavors is given by the following chain of inequalities,

$$\omega_{\rm cas}^{\max} > \omega_{\rm cas}^{\pi} > \frac{4\pi}{c}\int_E^\infty E' J_\nu(E')\,dE' > \frac{4\pi}{c} E J_\nu\ (> E),$$

where $\omega_{\rm cas}^{\max}$ and $\omega_{\rm cas}^{\pi}$ are the energy density of the cascade radiation allowed by the Fermi data and that produced only by pions, respectively. For the sake of comparison with experimental upper bounds, where an E^{-2} neutrino spectrum is usually assumed, we give the upper limit for the differential cosmogenic neutrino flux of three neutrino flavors with an E^{-2} spectrum and as function of the ratio of energy densities of pair- and pion-produced cascades $\omega_{\rm cas}^{e^+e^-}/\omega_{\rm cas}^{\pi}$,

$$E^2 J_\nu(E) \leqslant \frac{c}{4\pi}\,\frac{\omega_{\rm cas}^{\max}}{\ln(E_{\max}/E_{\min})}\,\frac{1}{1+\omega_{\rm cas}^{e^+e^-}/\omega_{\rm cas}^{\pi}}. \qquad (6)$$

This limit is plotted in Fig. 3 as a red line labeled 'E^{-2} cascade' together with existing upper limits from various experiments and the expected sensitivity of IceCube and JEM-EUSO [18,19]. Eq. (6) gives the general upper limit on the neutrino flux using the E^{-2} assumption. However, each particular model for cosmogenic neutrinos can be checked for consistency with the Fermi bound straightforwardly, as described in Section 2. Namely, $\omega_{\rm cas}$ can be calculated from Eq. (5) and compared with $\omega_{\rm cas}^{\max} = 5.8\times 10^{-7}$ eV/cm^3.

We discuss now the impact of magnetic fields on the cascade limit. In the presence of magnetic fields, the energy of electrons is partly dissipated in the form of synchrotron radiation. The critical energy $E_e^{\rm cr}$ of electrons above which synchrotron energy losses dominate is determined by the relation $(dE/dt)_{\rm syn} = (dE/dt)_{\rm IC}$, where the indices 'syn' and 'IC' are related to synchrotron and IC losses, respectively.

In the case of a single electron with energy $E_0 > E_e^{\rm cr}$, the usual electromagnetic cascade is suppressed until the electron energy drops below $E_e^{\rm cr}$. In this case, the total cascade energy is reduced by the factor $E_e^{\rm cr}/E_0$ compared to the case without magnetic field. However, the cascade is initiated by many electrons with production spectrum $\propto E_e^{-2}$, as required for an E_ν^{-2} upper limit. Then the cascade energy density $\omega_{\rm cas}(E_e)\,dE_e$ is proportional to $E_\nu J_\nu(E_\nu)\,dE_\nu$, and the ratio of the cascade energy density in

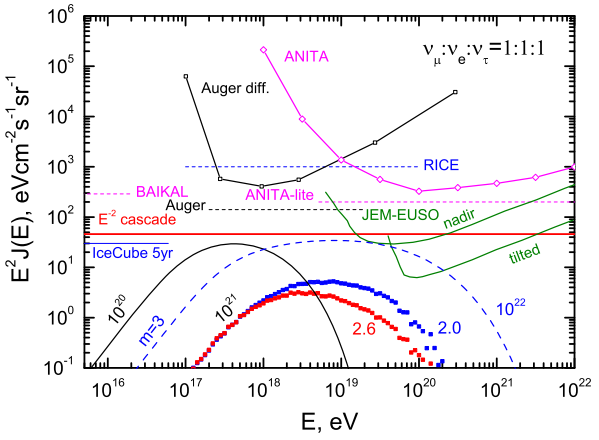

Fig. 3. Upper limits on the all-flavor UHE neutrino flux and expected sensitivities [18] together with the cascade limit ("E^{-2} cascade"). Also shown are realistic fluxes of cosmogenic neutrinos marked by their spectral index $\alpha_g = 2.6$ (dip model) and $\alpha_g = 2.0$ (ankle model) together with neutrino fluxes optimized for detection by IceCube and JEM-EUSO (as described in Section 4), which marked in the figure by their respective $E_{\max}$ values in eV (10^{20} and 10^{22}). (For interpretation of the references to color in this figure, the reader is referred to the web version of this Letter.)

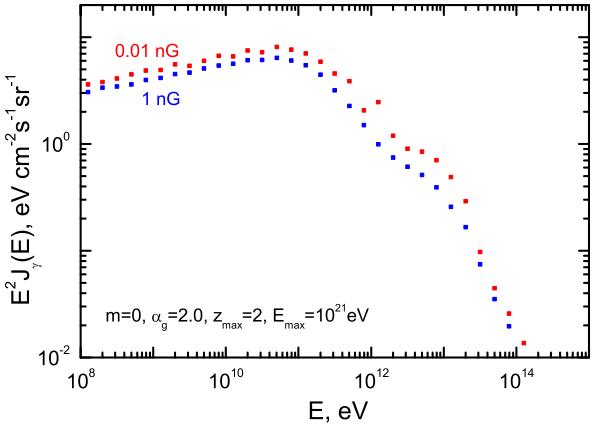

Fig. 4. Photon fluxes from the Monte Carlo simulation for different magnetic field strengths $B = 0.01$ and 1 nG with $E_{\max} = 10^{21}$ eV, $z_{\max} = 2$, $m = 0$ and $\alpha_g = 2.0$.

presence of a magnetic field $\omega_{\rm cas}^B$ and in its absence $\omega_{\rm cas}$ is given by

$$\frac{\omega_{\rm cas}^B}{\omega_{\rm cas}} = \frac{\ln(E_e^{\rm cr}/E_e^{\min})}{\ln(E_e^{\max}/E_e^{\min})}. \qquad (7)$$

For the case of a strong magnetic field $B \sim 1$ nG one obtains $E_e^{\rm cr} \sim 2\times 10^{18}$ eV. Taking $E_{\max} \sim 1\times 10^{21}$ eV and $E_{\min} \sim 1\times 10^{9}$ eV, we find $\omega_{\rm cas}^B/\omega_{\rm cas} = 0.78$, i.e. only 22% of the cascade energy is lost due to synchrotron radiation.

The case considered above corresponds to the E^{-2} upper limit shown in Fig. 3. For cosmogenic neutrinos produced by protons interacting with CMB the fraction of energy lost from the cascade is less because of the steeper generation spectrum $Q_p(E) \propto E^{-\beta_g}$ with $\beta_g \sim 2.3$–2.7. As a result the cascade energy is produced mainly by low-energy electrons, for which IC dominates. The ratio (7) is given now by

$$\frac{\omega_{\rm cas}^B}{\omega_{\rm cas}} = \frac{1-(E_e^{\rm cr}/E_{\min})^{-(\beta_g-2)}}{1-(E_{\max}/E_{\min})^{-(\beta_g-2)}}, \qquad (8)$$

and is for all practical cases very close to 1. Our photon fluxes from MC simulations with $B = 0.01$ and 1 nG displayed in Fig. 4 show

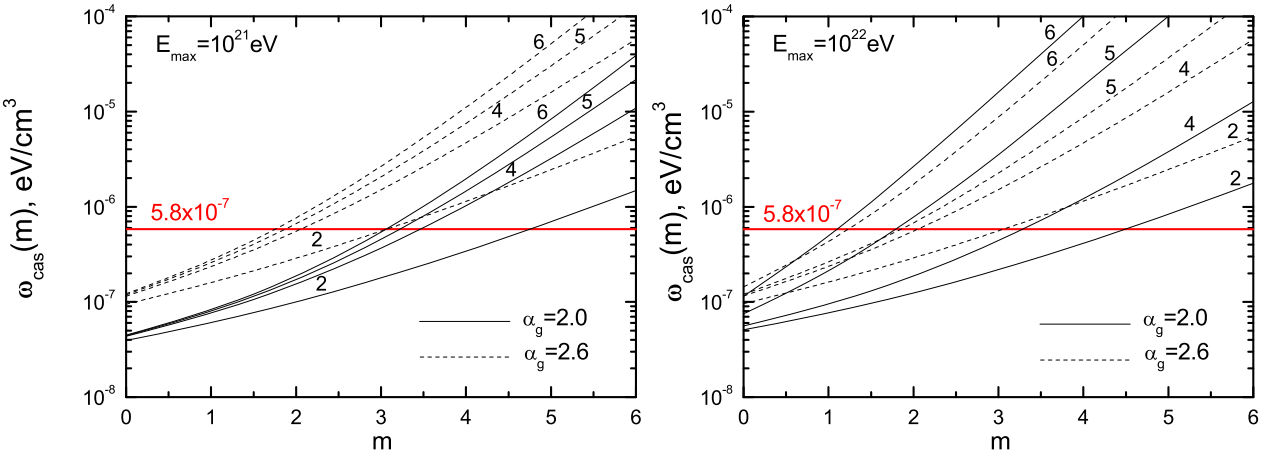

Fig. 5. Range of allowed evolution parameters, m and $z_{\max}$, for extended reference models with fixed $E_{\max} = 1 \times 10^{21}$ eV (left panel) and $E_{\max} = 1 \times 10^{22}$ eV (right panel). The cascade energy density $\omega_{\rm cas}$ is shown as function of m by the solid lines for the ankle model ($\alpha_g = 2.0$), and dashed lines for the dip model ($\alpha_g = 2.6$). The numbers on the lines show $z_{\max}$. The allowed parameters correspond to part of the curves below $\omega_{\rm cas}^{\max} = 5.8 \times 10^{-7}$ eV/cm^3 shown by the red horizontal line. (For interpretation of the references to color in this figure legend, the reader is referred to the web version of this Letter.)

indeed only minor differences, compatible with the analytical estimate given above.

5. Cosmogenic UHE neutrino fluxes

We discuss now the cosmogenic neutrino fluxes compatible with the two conditions that the parent proton fluxes provide a good fit to the HiRes data and that the resulting EGRB respects the cascade bound. The latter is imposed by requiring that $\omega_{\rm cas}$ calculated with the help of Eq. (5) is smaller than $\omega_{\rm cas}^{\max}$ deduced from the Fermi data.

We begin with our reference models, given by the dip ($\alpha_g = 2.6$) and ankle ($\alpha_g = 2.0$) model normalized to the HiRes data, and using $E_{\max} = 1.0 \times 10^{21}$ eV, $z_{\max} = 2$ and non-evolution. These are conservative models which give in case of $\alpha_g = 2.6$–2.7 the lowest neutrino fluxes for the proton-dominated mass composition. These fluxes labeled in Fig. 3 by the generation indices 2.0 and 2.6 are shown in the central part of the figure. They are undetectable by Auger and the planned detector JEM-EUSO.

Next we extend our reference models, allowing larger $E_{\max}$ and cosmological evolution. This results in higher neutrino fluxes, limited however still by $\omega_{\rm cas}$. The bounds on the parameters of these models are shown in Fig. 5. The two panels of this figure show for $E_{\max} = 1 \times 10^{21}$ eV (left panel) and $E_{\max} = 1 \times 10^{22}$ eV (right panel), how the two parameters describing source evolution, m and $z_{\max}$, are limited by $\omega^{\max} = 5.8 \times 10^{-7}$ eV/cm^3. Generally, strong evolution $(m, z_{\max})$ with $m \gtrsim 3$ and $z_{\max} \gtrsim 4$ is excluded, in accordance with the cases presented in Table 1. The evolution in the dip model ($\alpha_g = 2.6$) is restricted stronger, because of the increased contribution from e^+e^- pair-production.

The cosmogenic neutrino flux can become detectable only in the case of source evolution and large $E_{\max}$. Two extreme models of such neutrino fluxes are shown in the lower-right and lower-left corners of Fig. 3. Both models respect the bound from the observed UHECR flux and from $\omega_{\rm cas}^{\max}$ derived from the Fermi-LAT data, but use extreme values for the model parameters. Choosing the parameters for the model in the lower-right corner (the curve marked 10^{22}) we try to reach the sensitivity of JEM-EUSO. Since a soft spectrum increases $\omega_{\rm cas}$, we choose the hard spectrum with $\alpha_g = 2.0$, while $E_{\max}$ should be as large as possible. By other words we search for the extension of the ankle reference model with allowed evolution and large $E_{\max}$. We choose $E_{\max} = 1 \times 10^{22}$ eV, with $z_{\max} = 2$ and evolution parameter $m = 3$. Normalized to the HiRes data, this model has $\omega_{\rm cas} = 3.3 \times 10^{-7}$ eV/cm^3, i.e. is somewhat below the cascade limit (see also Fig. 5). For such values, the neutrino flux is marginally detectable by JEM-EUSO.

In the lower-left corner (the curve marked 10^{20}) we aim to cosmogenic neutrino detection by IceCube. Here we should increase the low-energy tail of the neutrino flux and suppress the pair-produced cascade radiation. To that end, we use $\alpha_g = 2.0$ with strong evolution to enhance the flux of low-energy neutrinos. The maximum acceleration energy can be low, e.g. $E_{\max} = 1 \times 10^{20}$ eV. Moreover, we choose evolution with $m = 3.0$ and $z_{\max} = 6.0$, which results in $\omega_{\rm cas} = 5.5 \times 10^{-7}$ eV/cm$^3 \approx \omega_{\rm cas}^{\max}$. As our calculations show, the flux is only marginally detectable by IceCube even for these extreme parameters.

The two models above demonstrate that even for extreme assumptions cosmogenic neutrinos remain undetectable by existing detectors such as Auger, and could be only marginally observed by IceCube and by future detectors JEM-EUSO and Auger-North (with sensitivity to neutrinos 5–6 times higher than Auger-South).

The observation of radio emission from neutrino-induced air showers provides an effective method for the detection of low fluxes of cosmogenic neutrinos from the highest energy part of their spectrum. The upper limit on UHE cosmogenic neutrino flux from the most restrictive experiment of this type, ANITA, is shown in Fig. 3 (Gorham et al. [18]). Recently, several particles with energies above 1×10^{19} eV have been detected there [20]. The high energy threshold is a disadvantage of this method. In the recently proposed ARIANNA detector [21], the threshold might be lowered to about 10^{17} eV while monitoring 900 km^2 of Antarctic ice.

A very sensitive instrument for UHE neutrino detection has been proposed in the project LORD (Lunar Orbital Radio Detector) [22], where a detector on a lunar satellite can observe the neutrino-produced radio-signal from lunar regolith. The sensitivity of this instrument, as estimated by the authors of the project, should be sufficient for the measurement of the cosmogenic neutrino fluxes shown in Fig. 3 by curves 10^{21}.

Before concluding, we would like to compare the results of this investigation to the ones of Ahlers et al. [23] that appeared after ours in the arXiv. While the main goal of our work was to derive an upper limit on the cosmogenic neutrino flux, the authors of Ref. [23] aimed at exploring the allowed parameter space of UHECR models, notably of those predicting maximal neutrino fluxes. These authors used as their criterion for the rejection of UHECR models $\omega_{\rm cas}^{\max} = 5.8 \times 10^{-7}$ eV/cm^3 from our calculations, and thus the

derived maximally allowed cosmogenic neutrino fluxes should coincide. The largest cosmogenic neutrino fluxes presented in Fig. 4 of Ref. [23] are very similar to our fluxes obtained in the extreme models with strong cosmological evolution (e.g. the curve 10^{22} in Fig. 3), both exceeding our reference cases ($\alpha_g = 2.6$ and $\alpha_g = 2.0$ without evolution) by an order of magnitude at $E \sim 10^{18}$–10^{19} eV. It is noteworthy that a much stronger cosmological evolution was considered in the calculations of Ref. [23]. Among other differences, the authors of Ref. [23] assumed that the IceCube sensitivity extends up to 10^{19} eV, while we used $E_{\max} = 10^{17}$ eV following Ref. [19].

6. Summary

We have used a recent measurement of the EGRB by Fermi-LAT to constrain models for UHECR and cosmogenic UHE neutrinos and to demonstrate that the latter are not detectable with the present experimental sensitivity. Both the dip and ankle models without or with weak evolution are consistent with the Fermi-LAT measurement of the EGRB. The cosmogenic neutrino flux is strongly limited by the new upper cascade bound and undetectable for a conservative choice of parameters by Auger-North and JEM-EUSO. Only for an extreme set of parameters, $E_{\max} \gtrsim 1 \times 10^{22}$ eV and $\omega_{\rm cas} \sim \omega_{\rm cas}^{\max}$, the cosmogenic flux is marginally detectable by JEM-EUSO. To achieve the observation of cosmogenic neutrinos for less extreme parameters, the detection threshold of JEM-EUSO (in the tilted mode) must be lowered down to 1×10^{19} eV and the sensitivity of Auger-North should be increased by factor ~ 20 in comparison with Auger-South. The further development of radio-detection methods gives another hope for detection of small fluxes of cosmogenic neutrinos.

The results of our Letter emphasize the necessity to develop more sensitive methods for the detection of cosmogenic neutrinos.

Acknowledgements

V.B. and A.G. are grateful to the ICTP, Trieste for hospitality. S.O. acknowledges a Marie Curie IEF fellowship. This work was partially supported by the program Romforskning of Norsk Forskningsradet.

References

[1] K. Greisen, Phys. Rev. Lett. 16 (1966) 748;
G.T. Zatsepin, V.A. Kuzmin, JETP Lett. 4 (1966) 78;
G.T. Zatsepin, V.A. Kuzmin, Pis'ma Zh. Eksp. Teor. Fiz. 4 (1966) 114.
[2] R. Abbasi, et al., HiRes Collaboration, Phys. Rev. Lett. 100 (2008) 101101.
[3] J. Abraham, et al., Pierre Auger Collaboration, Phys. Rev. Lett. 101 (2008) 061101.
[4] V.S. Beresinsky, G.T. Zatsepin, Phys. Lett. B 28 (1969) 423;
V.S. Beresinsky, G.T. Zatsepin, Sov. J. Nucl. Phys. 11 (1970) 111.
[5] V.S. Berezinsky, S.I. Grigor'eva, Astron. Astrophys. 199 (1988) 1.
[6] V. Berezinsky, A.Z. Gazizov, S.I. Grigorieva, Phys. Rev. D 74 (2006) 043005, astro-ph/0210095.
[7] V.S. Berezinsky, A.Yu. Smirnov, Astrophys. Sp. Sci. 32 (1975) 461;
For recent works see D.V. Semikoz, G. Sigl, JCAP 0404 (2004) 003;
Z. Fodor, S.D. Katz, A. Ringwald, H. Tu, JCAP 0311 (2003) 015;
K. Kotera, D. Allard, A.V. Olinto, arXiv:1009.1382.
[8] M. Ave, N. Busca, A.V. Olinto, A.A. Watson, T. Yamamoto, Astropart. Phys. 23 (2005) 19;
D. Hooper, A. Tailor, S. Sarkar, Astropart. Phys. 23 (2005) 11.
[9] A.A. Abdo, et al., Fermi-LAT Collaboration, arXiv:1002.3603 [astro-ph.HE].
[10] V.S. Berezinsky, et al., Astrophysics of Cosmic Rays, Elsevier, Amsterdam, 1990;
V.S. Berezinsky, Nucl. Phys. B 380 (1992) 478.
[11] F.W. Stecker, M.H. Salamon, Astrophys. J. 464 (1996) 600.
[12] A. Neronov, et al., Astrophys. J. Lett. 719 (2010) 130, arXiv:1002.4981 [astro-ph.HE].
[13] M. Kachelrieß, D. Semikoz, Astropart. Phys. 23 (2005) 486.
[14] A. Mücke, et al., Comput. Phys. Comm. 124 (2000) 290.
[15] For a calculation of the energy spectra of electrons see S.R. Kelner, F.A. Aharonian, Phys. Rev. D 78 (2008) 034013.
[16] M. Kachelrieß, S. Ostapchenko, R. Tomàs, New J. Phys. 11 (2009) 065017.
[17] T.M. Kneiske, et al., Astron. Astrophys. 413 (2004) 807.
[18] J. Abraham, et al., Pierre Auger Collaboration, Phys. Rev. Lett. 100 (2008) 211101;
P.W. Gorham, et al., ANITA Collaboration, arXiv:1003.2961 [astro-ph.HE];
I. Kravchenko, et al., Phys. Rev. D 73 (2006) 082002;
N. Inoue, K. Miyazawa, Y. Kawasaki, JEM-EUSO Collaboration, Nucl. Phys. B Proc. Suppl. 196 (2009) 135.
[19] J. Ahrens, et al., IceCube Collaboration, Astropart. Phys. 20 (2004) 507.
[20] S. Hoover, et al., arXiv:1005.0035 [astro-ph.HE].
[21] L. Gerhardt, et al., arXiv:1005.5193 [astro-ph.HE].
[22] G.A. Gusev, et al., Nucl. Instr. Methods A 604 (2009) S124;
V.A. Ryabov, et al., Nucl. Phys. B Proc. Suppl. 196 (2009) 458.
[23] M. Ahlers, et al., Astropart. Phys. 34 (2009) 106, arXiv:1005.2620.